Journal of New Materials for Electrochemical Systems 20, 175-181 (2017)

Controlled Synthesis of ZnO Nanostructures by Electrodeposition without Any Pretreatment and Additive Regent

Xin Xi[1,2], Chao Yang[1,2], Lei Liu[1,2], Shichao Zhu[1,2], Haicheng Chao[1,2] and Lixia Zhao[*,1,2]

[1]Semiconductor Lighting Research and Development Center, Institute of Semiconductors, Chinese Academy of Sciences, P. R. China
[2]College of Materials Science and Optoelectronic Technology, University of Chinese Academy of Sciences, Beijing 100049, People's Republic of China

Received: April 29, 2017, Accepted: July 30, 2017, Available online: September 25, 2017

Abstract: *ZnO nanostructures have been fabricated using electrodeposition method without any additive reagent and nucleation-layer. The influences of the applied voltage, temperature, electrolyte concentration, and time on the nanostructures of ZnO have been investigated using cyclic voltammety (CV), X-ray diffraction (XRD) and Scanning Electron Microscopy (SEM). The result shows that the 1-dimensional (1D) nanostructures tend to be formed at lower voltage and electrolyte concentration, while 2-dimentional (2D) nanostructures can be easily obtained at higher voltage and concentration. Although increasing temperature is helpful to grow 1D nanostructures, but excessive high temperature will destroy the ZnO nanostructures because of the high solubility of ZnO. Furthermore, we reveal the mechanism of the formation of ZnO nanostructures mainly depends on the competition between the hydroxylation and dehydration reaction. Our work is helpful for developing the photocatalytic and photodetection applications using different ZnO nanostructures.*

Keywords: ZnO, nanostructure, electrodeposition

1. INTRODUCTION

Zinc Oxide (ZnO) is a promising semiconductor with a direct wide bandgap (3.37eV) and large exciton energy (60mV)[1], which can be used in many optoelectronic devices, such as ultraviolet (UV) light-emitting diodes[2], photodetectors[3], gas sensors[4] and solar cells[5-7]. Till now, many different ZnO nanostructures including 1D nanostructures (nanocolumns[1,8], nanowires[9,10], nanotubes[11], nanorods[12]) and 2D nanostructures (nanoplates[13], nanoflowers[14], nanorings[15]) have been successfully synthesized using various methods. The reported optoelectronic properties of ZnO are strongly dependent on its growth condition because of the exposure of different crystal facets. For example, the {0001} polar facet can improve the photocatalytic property[16] and the $\{01\bar{1}0\}$ surface can be used to fabricate the ultrafast laser diode[17]. In general, the formation of different nanostructures is mainly determined by the ZnO growth along different crystal directions. The 1D nanostructures tend to be grown along the c-axis, whereas vertical to the c-axis for the 2D nanostructures[18]. The growth of the ZnO crystal naturally shows a anisotropic growth rate with $V[0001] > V[01\bar{1}0] > V[\bar{1}000]$[19]. Therefore, the ZnO crystals often exist as 1D nanostructures elongate along the c-axis by using the ordinary growth methods. However, with the increase of the nanorod length, the polar surface of the grown ZnO in 1D nanostructures would be continuously reduced because of the intrinsic crystal growth principle. Polar surface can serve as an active site for the photocatalytic reaction. Therefore, compared with the 2D nanostructures, the 1D nanostructures can reduce their photocatalytic properties[1] with the lengths increasing. But the large surface-to-volume ratio of ZnO 1D nanostructures can present high photosensitivity due to more surface trap states[3]. So synthesizing different ZnO nanostructures in controllable way is important for different photocatalytic and photodetector device applications.

Previously, 1D and 2D ZnO nanostructures have been synthesized using different technologies, including vapor-liquid-solid (VLS)[20], chemical vapor deposition (CVD)[21], molecule beam epitaxy (MBE)[22], metal organic chemical vapor deposition (MOCVD)[23], spray pyrolysis[24] and pulsed-laser deposition[25]. But these methods are often implemented either using

*To whom correspondence should be addressed: Email: lxzhao@semi.ac.cn

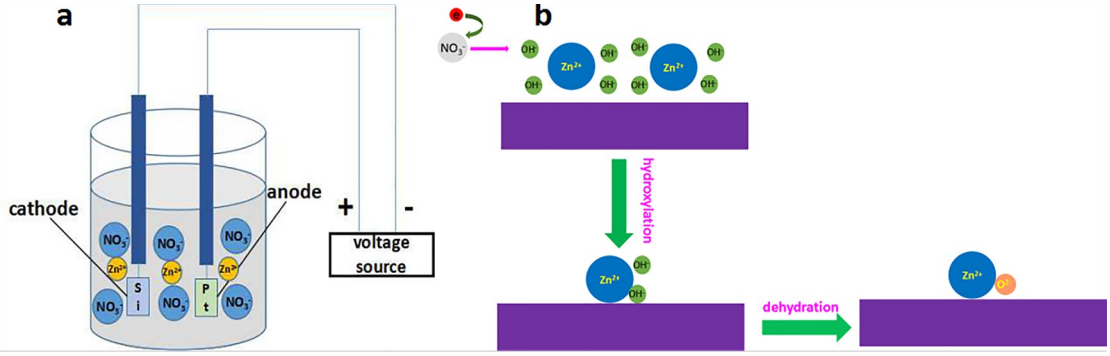

Figure 1. Schematic illustration of ZnO electrodeposition setup a) and the formation process of ZnO b).

complicated instruments, noble catalysts, or at high temperatures which result in a high cost for the ZnO fabrication. Electrodeposition has been reported as an efficient method, which can grow ZnO at low temperature, with large-scale fabrication and low cost[26,27].

The electrochemical synthesis of ZnO is normally carried out in an aqueous solution containing the Zn^{2+} ions and precursor of OH^-. Firstly, the precursor is reduced to OH^- electrochemically, which will react with Zn^{2+} to form the $Zn(OH)_2$ precipitation. Then, the $Zn(OH)_2$ will dehydrate to the final product of ZnO[8]. In previous work, almost all of the ZnO nanostructures grown by electrodeposition process need to use the additive reagents and pretreatments on the substrate. And it proved that the ZnO nanostrutures have been strongly influenced by the additive reagents[28,29], type of substrates[1,9] and pretreatments on the substrate[7,10], etc[30,31]. For example, Mohammad *et al*.[8] reported that the 1D ZnO nanostructures had been successfully synthesized with tunable diameters and lengths by controlling the electrolytic parameters after the deposition of a seed layer. Bin Fang *et al*.[14] synthesized the 1D ZnO nanostructures with different sizes using KCl as additive reagent. However, most studies on the electrodeposition only focused on the 1D nanostructures, few work has been done on the 2D nanostructures synthesis using the electrodeposition process. Although the 1D nanostructures can have large surface to volume ratio which result in the high photoresponsivity, the 2D nanostructures can increase the polar surface and improve the photocatalytic property. Moreover, the additive reagents and pretreatments on the substrate are indispensable in most electrodeposition fabrication work, which will make the process more complicated. In addition, the mechanism between the different nanostructures and growth conditions has not been clarified and more precise control in the electrodeposition process need to be explored to fabricate the ZnO nanostructures in a controllable way.

In this study, without any pretreatment and additive regent, different ZnO nanostructures have been successfully synthesized including nanowires, nanospikes and nanoplates. Our results show that at the lower voltage and electrolytic concentration, 1-dimensional (1D) ZnO nanostructures is formed, while at the higher voltage and concentration, 2-dimentional (2D) nanostructures are mainly obtained. In addition, higher temperature is helpful to grow 1D ZnO nanostructures, but excessive high temperature will destroy the ZnO nanostructure because of the high solubility of ZnO. Furthermore, we investigate the formation mechanism for different ZnO nanostructures and find that the formation of ZnO nanostructure mainly depends on the competition between the hydroxylation and dehydration. Our work shows a controllable way to grow different ZnO nanostructures without any additive reagents and pretreatments on the substrate, which is important for developing ZnO based photocatalysts and photodetector devices.

2. EXPERIMENTAL

All the chemical reagents used in our experiment were of analytic grade without any further purification. The electrodeposition system was carried out in a three-electrode system using chi660e electrochemical workstation as power source, as shown in figure 1-a. The $Zn(NO_3)_2$ was used as electrolyte without any additive reagent. Except for cleaning, no further pretreatment was performed to the silicon substrate, and the counter electrode was a Pt filament with an area of 2.0×2.0 cm^2. A saturated calomel electrode (SCE) was used as the reference electrode. The atmosphere temperature was controlled by an electro-thermostatic water cabinet.

Before the electrodeposition process, the substrate was ultrasonically rinsed in acetone and ethanol separately for fifteen minutes to remove the organic pollutants on the surface. Then, the substrate was cleaned by deionized water to wipe off the residual organic reagents. During the electrodeposition process, we carefully investigated how the applied voltage, temperature, time, and concentration of $Zn(NO_3)_2$ impact the growth of ZnO nanostructures. After the electrodeposition process, the obtained ZnO nanostructures on the substrate were rinsed using deionized water and dried in a drying cabinet at 60 ºC.

The electrodeposition process and cyclic votalmmety (CV) curve were carried out by the CHI660e potansiostat/galvanostat. Scanning electron microscopy (SEM) (Hitachi S4800) was used to examine the surface nanostructures of the samples. Crystal structure of the nanostructures was characterized using a Bruker D8 X-ray diffractometer equipped with Cu Kα line (λ = 0.15419 nm) radiation.

3. RESULTS AND DISCUSSION

There are three stages to form ZnO nanostructures during the cathodic electrodeposition process in zinc nitrate electrolyte. As illustrated in figure 1-b, firstly, the NO_3^- ions acquire electrons

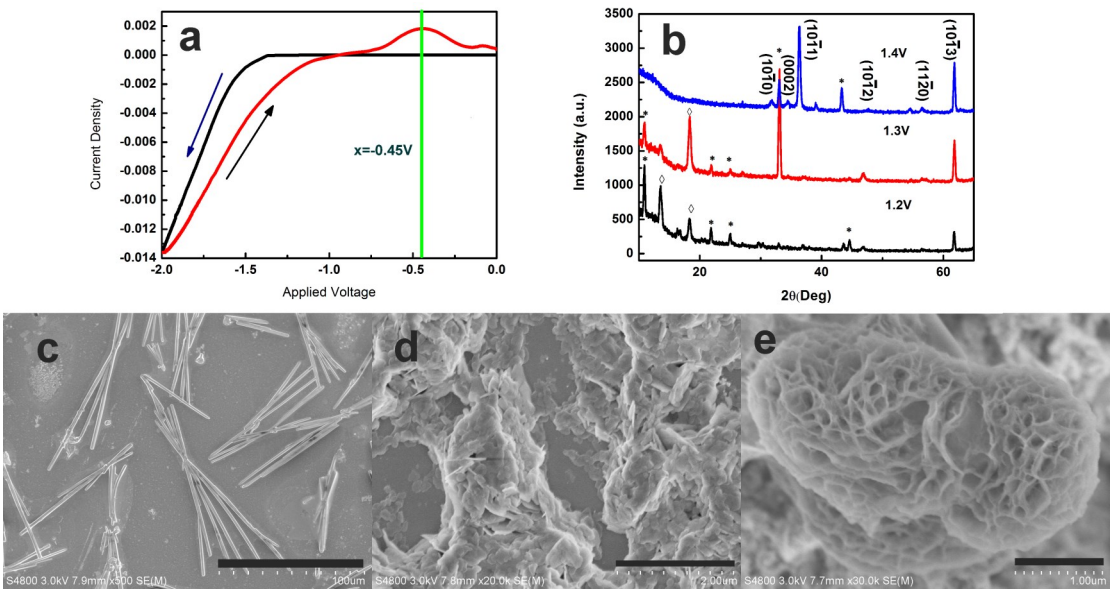

Figure 2. a) Cyclic voltammetry scans obtained during the formation of ZnO on the Si substrate using sweeping rate of Vb=10mV/s b) XRD patterns of ZnO generated at different voltages, stars (*) represent for the impurity of $Zn(NO_3)_2$, diamonds (◊) represent for the impurity of Zn(OH)2. SEM images of ZnO grown on the Si substrate at different voltages are illustrated in c) -1.2V, d) -1.3V, e) -1.4V.

from cathode and are reduced to NO_2^-, which generate the OH^- ions in the electrolyte (Reaction (1)). The generated OH^- ions will combine with Zn^{2+} ions and form an intermediate products of $Zn(OH)_2$ precipitations (Reaction (2)). Due to heat convection, diffusion of ions, and deregulation movement among molecules and ions in solution, the ZnO products are finally obtained by a dehydration process of $Zn(OH)_2$ (Reaction (3)). The whole reaction process can be generally expressed as Reaction (4).

$$NO_3^- + H_2O + 2e^- \rightarrow NO_2^- + 2OH^- \quad (1)$$

$$Zn^{2+} + 2OH^- \rightarrow Zn(OH)_2 \quad (2)$$

$$Zn(OH)_2 \rightarrow ZnO + H_2O \quad (3)$$

$$Zn^{2+} + NO_3^- + 2e^- \rightarrow ZnO + NO_2^- \quad (4)$$

During the ZnO electrodeposition process, all the parameters, such as temperature, voltage, $Zn(NO_3)_2$ concentration and time can change the ZnO nanostructures due to their influence on the changes of reaction rate, ions mobility and reactants concentration. Hence, we carried out experiments under different conditions to investigate the influence of the growth condition on the morphology of ZnO nanostructures during the electrodeposition process.

3.1. The influence of the applied voltage

The influence of the applied voltage on the ZnO nanostructures was studied in 0.1mol/L $Zn(NO_3)_2$, directly on the Si substrate at 20 °C. The cyclic voltammetry (CV) method which scanned cathodically 10 mV/s was performed over the potential range from 0 V and -2 V, as shown in figure 2 a).

An obvious current droop is located at -1.3 V which corresponds to the beginning of the reduction of NO_3^-. This potential is more negative than the thermodynamically value of -0.46V[32]. This retardation is mainly due to the potential difference between the negatively charged surface and the Zn^{2+} concentration close to the cathode. An additional anodic peak (E=-0.45V) was observed during the backward scan, which suggests the formation of metallic zinc on the cathode[33]. Because an obvious dropdown of the current density which represent the initiation of electrodeposition of ZnO occurred at about -1.2 V, three different voltages of -1.2 V, -1.3 V, and -1.4 V were selected as the voltage parameters to investigate the influence of applied voltage on the nanostructures of ZnO.

Figure 2 b) shows the XRD patterns at different voltages. At -1.2 V, the products were composed of mixtures contained $Zn(OH)_2$, $Zn(NO_3)_2$ and ZnO with low crystallinity. At -1.3 V, the crystal quality of the products becomes better and the peak at the (0002) crystal facet starts to appear. Increasing the voltage to -1.4 V, the crystallinity gets even higher and the crystal growth direction starts to grow along the $(10\bar{1}1)$ which results in the 2D nanosheet structure. The corresponding SEM images are shown in figure 2 c-e). The nanostructures of the ZnO tend to be nanowires at -1.2 V, adhesive thick plates at -1.3 V and nanosheet structure at -1.4 V, which are consistent with the XRD results.

The formation of the ZnO nanostructures in the electrodeposition is mainly composed of two processes, hydroxylation and dehydration, as illustrated by the reactions (2) and (3). The higher voltage applied to the cathode can enhance the reduction reaction of the NO_3^- in the electrolyte, which will generate more OH^- ions to the cathode. Meanwhile, the more negatively charged cathode can attract more Zn^{2+} in the electrolyte near the cathode, which will accelerate the formation of $Zn(OH)_2$. The more OH^- and Zn^{2+} will lead to a relative higher hydroxylation reaction speed. When the dehydration rate (k_{dedydr}) is slower than the hydroxylation rate (k_{hydrox}) ($k_{dedydr} < k_{hydrox}$), the ZnO will form in 2D nanostructures (nanoplates or nanosheets structure). On the contrary, lower voltage

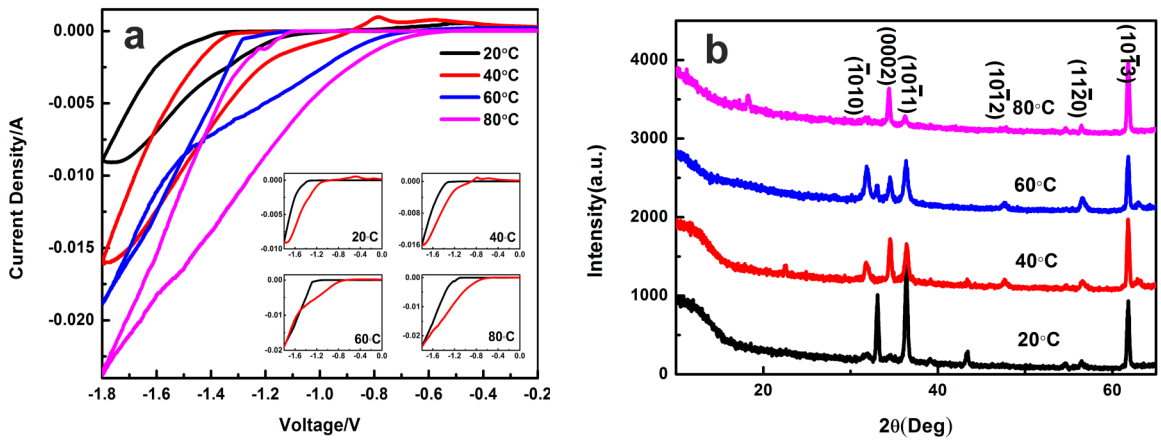

Figure 3. a) Cyclic voltammetry scans obtained during the formation of ZnO on Si substrate at different temperatures using sweeping rate of Vb=10mV/s, b) XRD patterns of ZnO generated at different temperatures.

will reduce the reduction reaction and attract less Zn^{2+} around the cathode, which would make the dehydration rate higher than hydroxylation rate ($k_{hydrox}<k_{dedydr}$), and result in the formation of the 1D nanostructures (nanowire).

3.2. The influence of the temperature

Different bath temperatures at 20, 40, 60 and 80°C were used to investigate the influence of temperature on the growth ZnO nanostructures. In the whole process, the $Zn(NO_3)_2$ concentration of the solution was 0.1 mol/L and the current density was fixed at 10^4 μA. Figure 3 a) shows the CV curves at different temperatures. The anodic peak for the reduction reaction of Zn^{2+} to metal Zn shifts backward and finally disappears with increasing the temperature.

The backward shift is mainly because the increase of the temperature which will enhance the reduction of the NO_3^- and generate more OH^- indirectly. These OH^- ions react with the Zn^{2+} directly and consequently break the chemical balance of generation of metal Zn, which make less Zn^{2+} be reduced to metal Zn and finally the reduction vanish.

Figure 3 b) shows the XRD patterns of ZnO deposited at different temperatures. The strong diffraction peak assigned to the ZnO (0002) can be clearly observed at higher deposition temperature, indicating the growth direction along c-axis (1D nanostructure). However, the $(10\bar{1}1)$ crystal facet at low temperature is stronger than high temperature, indicating the growth direction vertical to the c-axis (2D nanostructure). This trend measured by XRD patterns can also be confirmed by the SEM images, as shown in Figure 4. At temperature 20 °C, the ZnO electrodeposited on the Si substrate is a cluster of nanoplates (2D) constructed in porous quasi-columns with sharper peak at $(10\bar{1}1)$ in the XRD patterns. When the temperature increased to 40 °C, the nanoplates (2D) grew larger perpendicular to the substrate which corresponds to a little sharp peak of $(10\bar{1}1)$ in XRD patterns. Afterwards, the 2D nanostructures disappeared and transformed to nanospike (1D nanostructure) with a small peak $(10\bar{1}1)$ in the XRD patterns. With the temperature further increasing to 80°C, an aggregation of

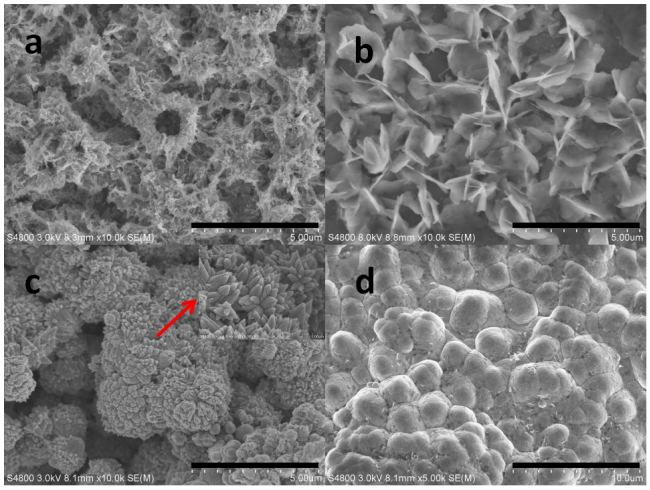

Figure 4. SEM of ZnO grown on the Si substrate at different temperatures, a) 20 ºC, b) 40 ºC, c) 60 ºC, d) 80 ºC.

ZnO nanoparticles started to form without any obvious nanostructure. This is mainly due to the high-solubility of ZnO in the electrolyte at high temperatures.

The strong impact of the temperature on the morphology of the ZnO nanostructures is mainly due to the different dehydration reaction rate at different temperatures. According to Arrhenius formula $k = A * e^{-E_a/kT}$ (where k is the reaction rate constant, A is a constant, E_a represents the reaction activation energy, R represents the molar gas constant and T represents the temperature), the dehydration reaction accelerates rapidly with the increase of the temperature. Therefore at lower temperatures, the dehydration reaction is slower. It makes the hydration reaction rate higher than dehydration reaction rate $k_{hydrox}>k_{dedydr}$, which will lead to the formation of 2D nanostructures. While with the temperature increasing, when the relative reaction rate becomes as $k_{hydrox}<k_{dedydr}$, the ZnO crystal will grow along the [0001] direction and result in the 1D nanostructures.

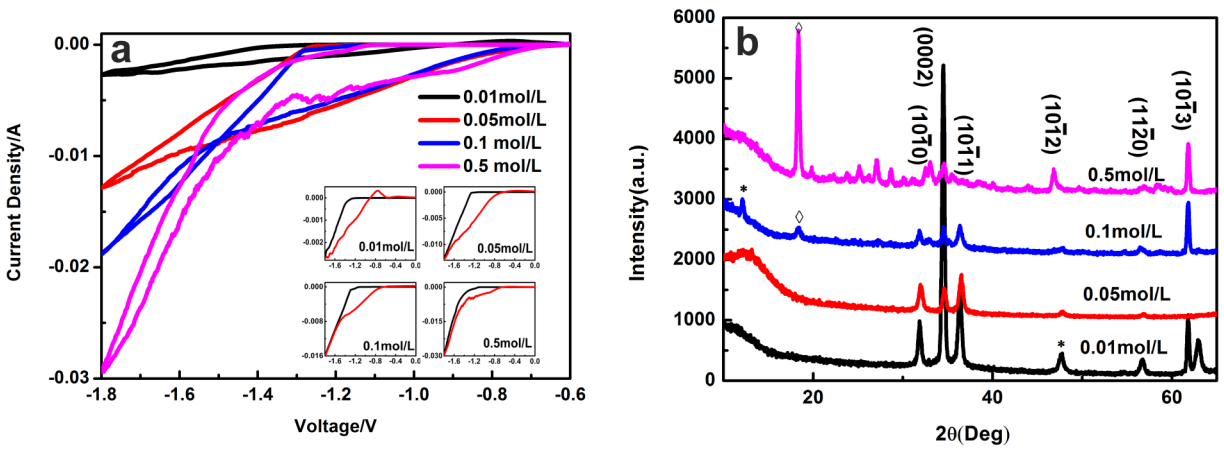

Figure 5. a) XRD patterns of ZnO generated at different $Zn(NO_3)_2$ concentration, b) Cyclic voltammetry scans obtained during the formation of ZnO on Si substrate at different $Zn(NO_3)_2$ concentration using sweeping rate of Vb=10mV/s.

3.3. The influence of the $Zn(NO_3)_2$ concentration

The influence of the $Zn(NO_3)_2$ concentration on the nanostructures of ZnO was investigated using four different $Zn(NO_3)_2$ concentrations at 0.01, 0.05, 0.1 and 0.5 mol/L. Other parameters during the electrodeposition were kept constant. The applied current in the solution was 1×10^4 μA, the temperature used in the electrolytic bath was 50°C and the electrodeposition time was set as 900 s. Figure 5 a) shows the CV curves for the electrodeposition with different $Zn(NO_3)_2$ concentrations. At the lowest concentration of 0.01 mol/L, the CV curve has a backward peak, which represents the reduction reaction of the Zn^{2+} to metal Zn. When the concentration becomes higher, the reduction peak disappears and only two smooth forward and backward scan curves are left. This is mainly because that the higher concentration of $Zn(NO_3)_2$ can generate more NO_3^- ions, which will in turn improve the reduction of NO_3^- to NO_2^-. At the same time, lots of OH^- ions are produced through the process, which enhance the recombination of Zn^{2+} and OH^-. The chemical potential for Zn^{2+} ions to generate $Zn(OH)_2$ increases with increasing the $Zn(NO_3)_2$ concentration, therefore, the reaction of the reduction of Zn^{2+} to metal Zn becomes weaker. Finally, the reduction peak for Zn^{2+} to metal Zn disappeared as the rapid increase of OH^-. Figure 5 b) shows the XRD patterns of the ZnO generated on different concentrations. All the peaks related to the ZnO become weaker and many impurities' peaks appear with increasing the electrolyte concentration.

Figure 6 shows the SEM figures of the ZnO synthesized at different concentrations. At the concentration of 0.01 mol/L $Zn(NO_3)_2$ solution (figure 6a), the generated ZnO particles shows a formation of nanospikes arranged in globular bunches (1D). When the concentrations increased to 0.05 mol/L, the morphology of ZnO deposited on the substrate turned to nanoplates (2D) perpendicular to the substrate. With the $Zn(NO_3)_2$ concentration further increased to 0.5mol/L, there was no obvious variation among the SEM images of the generated ZnO. But the thicknesses of the ZnO nanoplates became thicker with increasing the concentration of the $Zn(NO_3)_2$ solution. The increased thickness indicates that the higher concentration of Zn^{2+} and NO_3^- can help the growth of 2D nanostructures. It is mainly because the formation of 2D nanostructures will restrain the growth direction of ZnO and make the nanostructure inclined to grow vertical to the grown 2D nanostructure which increase the thickness of the nanoplates.

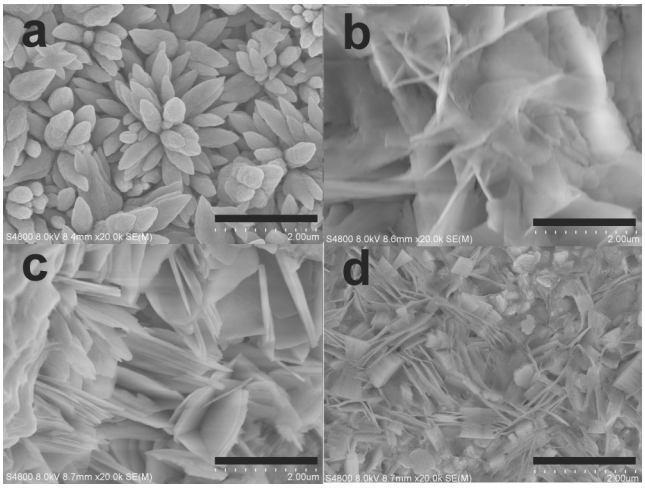

Figure 6. SEM of ZnO grown on the Si substrate at different $Zn(NO_3)_2$ concentrations, a) 0.01 mol/L, b) 0.05 mol/L, c) 0.1 mol/L, d) 0.5 mol/L.

At the higher concentration of $Zn(NO_3)_2$, more Zn^{2+} can be generated in the electrolyte which would accelerate the formation of $Zn(OH)_2$. The hydroxylation reaction is faster than the dehydration process. As discussed above, at a higher concentration of $Zn(NO_3)_2$ electrolyte, the solution will be more favorable to generate $Zn(OH)_2$ particles and the dehydration reaction cannot fulfill completely in the process. But in a lower concentration of $Zn(NO_3)_2$ solution, the generated $Zn(OH)_2$ particles can be dehydrated more sufficiently for the growth of ZnO. The dehydration rate has a great influence on the nanostructure of ZnO. For example, the fast dehydration reaction can effectively help the column formation for ZnO, otherwise the relative slow dehydration would form the nanoplates.

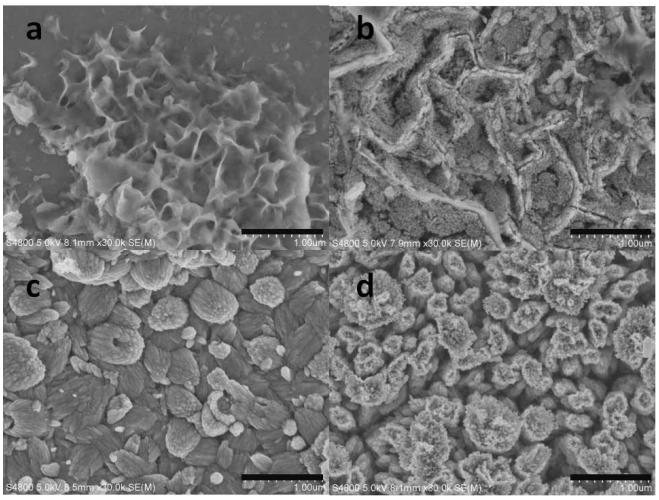

Figure 7. SEM of ZnO grown on the Si substrate at different time, a) 15 min, b) 30 min, c) 60 min, d) 120 min.

3.4. The influence of time

The deposition time on the morphologies of the ZnO nanostructures has also been examined with fixed $Zn(NO_3)_2$ concentration of 0.1 mol/L, applied current 1×10^{-4} A and bath temperature of 60 °C.

Figure 7 shows the SEM nanostructures electrodeposited at different time. Firstly, the morphology of ZnO is non-uniform nanoplates (2D) on the substrate. With the electrodepostion time increased to 30 min, the image of ZnO nanostructure exhibits a thicker ZnO wall with a rough surface. After the electrodeposition process for 60 min, the nanostructure of ZnO becomes bunches of ZnO clusters with nanorods (1D) and no further changes observed.

During the electrodeposition process, 2D ZnO nanostructures starts to grow on the substrate under 0.1mol/L $Zn(NO_3)_2$ concentration. With continuing the deposition time, the 2D nanostructures have electrodeposited between the nucleation to a large scale and cover up all the substrate. However, as the crystal continue to grow, the crystal growth based on the 2D nanostructures would limit the growth direction parallel the 2D facet and grow vertical to the substrate. Therefore, as the time further increasing, the ZnO grows perpendicular to the 2D nanostructures which will lead to the 1D nanostructures. The 1D ZnO growth starts from the bunches of ZnO nanowires to distributed nanowires which probably because the internal strain of the ZnO nanowires.

From above, different electrodeposition conditions have distinct influence on the nanostructure of ZnO. In general, the ZnO intends to grow along [0001] direction naturally during the electrodeposion process, which results in 1D nanostructures. However, the hydroxylation of Zn^{2+} will overcome the ZnO preferred growth direction and grow along $[10\bar{1}0]$ direction, which will result in 2D nanostructure. Therefore, these two reactions compete with each other to determine the final ZnO nanostructure in the electrodeposition process. When there are lots of OH^- and Zn^{2+} ions generated at the cathode, which will lead to a relative higher hydroxylation rate than the dehydration rate ($k_{hydrox}>k_{dedydr}$). On the contrary, less OH^- and Zn^{2+} around the cathode would allow the faster dehydration rate ($k_{hydrox}<k_{dedydr}$). When $k_{hydrox}>k_{dedydr}$, 2D nanostructures are inclined to grow but when $k_{hydrox}<k_{dedydr}$, 1D nanostructures will be formed, as illustrated in Figure 8. Therefore, at low voltage or using lower $Zn(NO_3)_2$ concentration, less OH^- and Zn^{2+} will generate at the cathode, which would result in 1D ZnO nanostructure. But using a high voltage or a high electrolyte concentration will allow to grow ZnO in 2D nanostructure.

4. CONCLUSION

Electrodeposition is a promising synthesis method to deposit ZnO with different nanostructures. By adjusting the voltage, temperature, $Zn(NO_3)_2$ concentrations in the process, ZnO with controllable nanostructures were successfully synthesized without any reagents and pretreatments on the substrate. The results show that the ZnO is inclined to form 1D nanostructure under lower electrolyte concentration or lower voltage. On the contrary, 2D nanostructure will be obtained under high electrolyte concentration or high voltage. Using high deposition temperature will lead to the formation of ZnO nanostructures from the 2D to 1D nanostructure. But the excessive higher temperature will make a condenser nanostructure because of the higher solubility in the electrolyte. The key factor to determine the nanostructure during the electrodeposition process is the competition between the hydroxylation and dehydration mechanism. When the $k_{hydrox}>k_{dedydr}$, the ZnO pre-

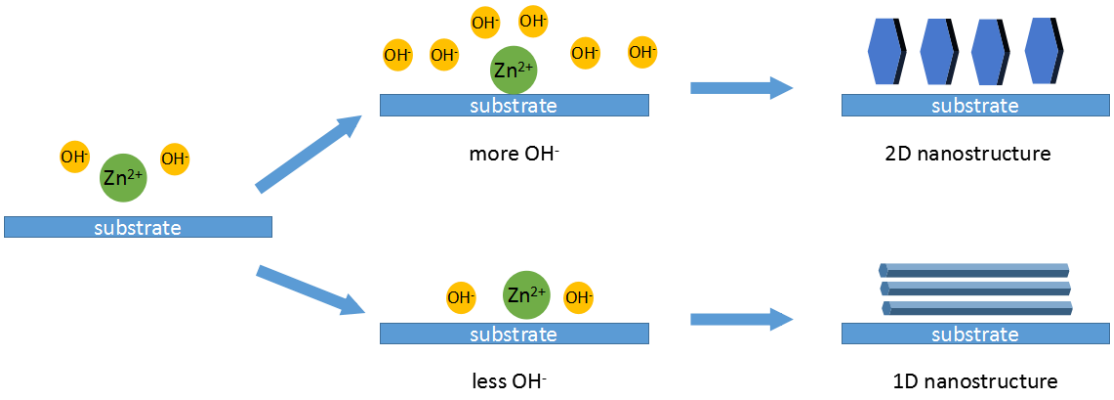

Figure 8. The mechanism for ZnO formation with different morphologies.

fer to grow in 2D nanostructure. Otherwise, the 1D nanostructure will be formed.

5. ACKNOWLEDGEMENTS

This work was supported by the National Natural Science Foundation of China (11574306), and the National Basic Research and High Technology Program of China (2015AA03A101, 2014BAK02B08 and 2015AA033303)

REFERENCES

[1] A. Simimol, P. Chowdhury, S. Ghosh, H.C. Barshilia, Electrochimica Acta, 90, 514 (2013).

[2] J. Huang, M.M. Morshed, Z. Zuo, J. Liu, Applied Physics Letters, 104, 131107 (2014).

[3] C. Soci, A. Zhang, B. Xiang, S.A. Dayeh, D. Aplin, J. Park, X. Bao, Y.H. Lo, D. Wang, Nano Letters, 7, 1003 (2007).

[4] P. Rai, S. Raj, K.J. Ko, K.-K. Park, Y.T. Yu, Sensors and Actuators B: Chemical, 178, 107 (2013).

[5] N.R. Farley, C.R. Staddon, L. Zhao, K.W. Edmonds, B.L. Gallagher, D.H. Gregory, Journal of Materials Chemistry, 14, 1087 (2004).

[6] S. Shinde, C. Bhosale, K. Rajpure, Journal of Semiconductors, 34, 043002 (2013).

[7] M.Y.A. Rahman, A. Umar, R. Taslim, M.M. Salleh, Electrochimica Acta, 88, 639 (2013).

[8] M.R. Khajavi, D.J. Blackwood, G. Cabanero, R. Tena-Zaera, Electrochimica Acta, 69, 181 (2012).

[9] Y.H. Ko, M.S. Kim, J.S. Yu, Applied Surface Science, 259, 99 (2012).

[10] G. Nagaraju, Y.H. Ko, J.S. Yu, Materials Chemistry and Physics, 149, 393 (2015).

[11] Y. Sun, G.M. Fuge, N.A. Fox, D.J. Riley, M.N. Ashfold, Advanced materials, 17, 2477 (2005).

[12] K. Zarebska, M. Kwiatkowski, M. Gniadek, M. Skompska, Electrochimica Acta, 98, 255 (2013).

[13] D. Pradhan, K.T. Leung, Langmuir, 24, 9707 (2008).

[14] B. Fang, C. Zhang, W. Zhang, G. Wang, Electrochimica Acta, 55, 178 (2009).

[15] X.Y. Kong, Y. Ding, R. Yang, Z.L. Wang, Science, 303, 1348 (2004).

[16] E.S. Jang, J.H. Won, Y.W. Kim, X. Chen, J.H. Choy, Cryst. Eng. Comm., 12, 3467 (2010).

[17] J.C. Deinert, D. Wegkamp, M. Meyer, C. Richter, M. Wolf, J. Stähler, Physical review letters, 113, 057602 (2014).

[18] B. Cao, W. Cai, The Journal of Physical Chemistry C, 112, 680 (2008).

[19] P.X. Gao, C.S. Lao, Y. Ding, Z.L. Wang, Advanced Functional Materials, 16, 53 (2006).

[20] P. Yang, H. Yan, S. Mao, R. Russo, J. Johnson, R. Saykally, N. Morris, J. Pham, R. He, H.J. Choi, Advanced Functional Materials, 12, 323 (2002).

[21] S. Faÿ, L. Feitknecht, R. Schlüchter, U. Kroll, E. Vallat-Sauvain, A. Shah, Solar Energy Materials and Solar Cells, 90, 2960 (2006).

[22] M. Ying, W. Cheng, X. Wang, B. Liao, X. Zhang, Z. Mei, X. Du, S.M. Heald, H.J. Blythe, A.M. Fox, Materials Letters, 144, 12 (2015).

[23] Y. Liu, C. Gorla, S. Liang, N. Emanetoglu, Y. Lu, H. Shen, M. Wraback, Journal of Electronic Materials, 29, 69 (2000).

[24] S. Shinde, G. Patil, D. Kajale, V. Gaikwad, G. Jain, Journal of Alloys and Compounds, 528, 109 (2012).

[25] T. Shimogaki, M. Takahashi, M. Yamasaki, T. Fukuda, M. Higashihata, H. Ikenoue, D. Nakamura, T. Okada, Journal of Semiconductors, 37, 023001 (2016).

[26] X. Bai, L. Yi, D.L. Liu, E.Y. Nie, C.L. Sun, H.H. Feng, J.J. Xu, Y. Jin, Z.F. Jiao, X.S. Sun, Electrodeposition from ZnO nanorods to nano-sheets with only zinc nitrate electrolyte and its photoluminescence, Applied Surface Science 257 (2011) 10317-10321.

[27] Y. Lin, J.Y. Yang, X.Y. Zhou, Controlled synthesis of oriented ZnO nanorod arrays by seed-layer-free electrochemical deposition, Applied Surface Science 258 (2011) 1491-1494.

[28] L.F. Xu, Y. Guo, Q. Liao, J.P. Zhang, D.S. Xu, Morphological control of ZnO nanostructures by electrodeposition, J Phys Chem B 109 (2005) 13519-13522.

[29] D. Pradhan, K. Leung, Vertical Growth of Two-Dimensional Zinc Oxide Nanostructures on ITO-Coated Glass: Effects of Deposition Temperature and Deposition Time, The Journal of Physical Chemistry C 112 (2008) 1357-1364.

[30] S. Sun, S. Jiao, K. Zhang, D. Wang, S. Gao, H. Li, J. Wang, Q. Yu, F. Guo, L. Zhao, Journal of Crystal Growth, 359, 15 (2012).

[31] N. Orhan, M. Baykul, Solid-State Electronics, 78, 147 (2012).

[32] N. Kıcır, O. Ozkendir, A. Farha, F. Kırmızıgül, T. Tuken, C. Gumus, S. Çabuk, M. Erbil, Y. Ufuktepe, Indian Journal of Physics, 89, 1013 (2015).

[33] J. Elias, R. Tena-Zaera, C. Lévy-Clément, Thin Solid Films, 515, 8553 (2007).